

# Intra-Articular Cartilage Calcification Associated with Type II Pro-Collagen Accumulation in Chondrocytes and Abnormal Fibrils in the Extra Cellular Matrix (ECM): Case Report

Peter Storgaard Skagen, Tom Nicolaisen

Department of Sports Traumatology, Frederikssund Hospital, Frederikssund, Denmark

Email: pebsicola@yahoo.dk

**How to cite this paper:** Skagen, P.S. and Nicolaisen, T. (2019) Intra-Articular Cartilage Calcification Associated with Type II Pro-Collagen Accumulation in Chondrocytes and Abnormal Fibrils in the Extra Cellular Matrix (ECM): Case Report. *Case Reports in Clinical Medicine*, 8, 62-86. <https://doi.org/10.4236/crcm.2019.84009>

**Received:** February 11, 2019

**Accepted:** April 15, 2019

**Published:** April 18, 2019

Copyright © 2019 by author(s) and Scientific Research Publishing Inc. This work is licensed under the Creative Commons Attribution International License (CC BY 4.0). <http://creativecommons.org/licenses/by/4.0/>



Open Access

## Abstract

**Objective:** The purpose of this case-study was to perform morphological and molecular analysis of articular cartilage biopsies from the femoral condyle of a 33 year old woman with intra-articular calcification in the right knee joint and compare the findings with those of normal cartilage. **Methods:** Femoral condyle cartilage biopsies were used for Light Microscopy (LM), Transmission Electron Microscopy (TEM), explant culturing and DNA mutation analysis of the *COL2A1* gene. **Results:** X-ray of the affected knee joint showed intra-articular calcifications on the femur condyle, tibia and meniscus. Pathological LM and TEM examination of cartilage biopsies revealed calcified islands morphologically identical to calcium pyro-phosphate dehydrate (CPPD) and hydroxyapatite (HA)-like crystals. In addition, chondrocytes showed accumulation of pro-collagen molecules. With explant culturing and immunohistochemistry, it was confirmed that matrix calcification correlated with high intracellular matrix accumulation and expression of type X collagen. The induction of hypertrophy in chondrocytes was further associated with matrix vesicle (MV) release and a prominent calcification zone. Surprisingly, TEM showed crystal development on thick abnormal type II collagen fibrils suggesting that these ECM components might nucleate and contribute to calcification. **Conclusions:** We suggest that intra-articular calcification may be associated with type II pro-collagen accumulation in chondrocytes. In particular, we hypothesize that matrix accumulation may induce hypertrophy and type X collagen expression in cartilage cells and release of MV's into the ECM, which together with thick abnormal type II collagen hetero-fibrils, are responsible for crystal deposition in the ECM.

---

## Keywords

Calcification, Collagen Bundles, Endoplasmic Reticulum Storage Disease (ERSD)

---

## 1. Introduction

In tissues such as articular cartilage in which calcification is abnormal, previous studies [1] [2] [3] have confirmed that pathological Chondrocalcinosis is associated with deposition of non-urate crystals such as calcium pyrophosphate dehydrate (CPPD) and basic calcium phosphate (BCP) including hydroxyapatite (HA), in the knee joints.

This is particularly so in osteoarthritis (OA), where crystals of calcium salts are found in the knee joint fluid of up to 65% of OA patients [4] [5] and predict an increased severity of arthritis and a worsening progression of OA. In particular, studies have found both insoluble rhomboid CPPD crystals ( $\text{Ca}_2\text{P}_2\text{O}_7 \cdot 2\text{H}_2\text{O}$ ) and ultramicroscopic crystalline substances like BCP crystals including hydroxyapatite ( $\text{Ca}_{10}(\text{PO}_4)_6(\text{OH})_2$ ), octa-calcium phosphate ( $\text{Ca}_8(\text{HPO}_4)_2(\text{PO}_4)_4 \cdot 5\text{H}_2\text{O}$ ), tri-calcium phosphate ( $\text{Ca}_3(\text{PO}_4)_2$ ) and magnesium whitlockite ( $\text{Ca}_9(\text{Mg}, \text{Fe})(\text{PO}_4)_6\text{PO}_3\text{OH}$ ) [6] in articular cartilage, meniscus tissue, and synovial fluid from patients with OA [7] [8] [9]. It was shown in one study that about 95% of cartilage calcification involving hyaline cartilage in the knee was related to CPPD and BCP crystals [10].

Despite the evidence for a contribution of calcification to the pathogenesis of OA and the fact that there are differences in their clinical patterns [11] [12] [13], the mechanisms underlying development of these crystalline deposits are still not known. However, recent work has highlighted some important findings in this field, namely that abnormal hypertrophic chondrocytes in OA cartilage play a critical role in the development of both CPPD and BCP deposition by releasing matrix vesicles (MV) from the plasma membrane, providing a sheltered environment for the initiation of calcification [14] [15]. How the MV perform this function remains unknown although stable phenotype MV which are unable to calcify have also been found in normal articular cartilage, whereas they calcify primarily in cartilage from the joints of OA patients where they are responsible for both the initial formation of HA [15] [16] [17], and CPPD deposition [18] [19] [20]. In addition, CPPD crystals are rarely found in areas of normal articular cartilage matrix [21] but MV isolated from articular cartilage of OA patients do not have a greater capacity for crystal formation than MV isolated from normal cartilage [18] [19]. These findings suggest that alterations in matrix composition of the ECM may also have a role in the formation of crystalline deposits.

There are reports describing a link between type II collagen disease and intra-articular calcification in 4 families in Chiloe Islands [22] [23] [24], United States [25] and Finland [26]. Family members express a clinical phenotype of OA due to an Arg<sup>75</sup>-Cys mutation within the *COL2A1* gene coding for type II

pro-collagen. This genetic disease was associated with childhood-onset OA and linked to intra- and extra-articular calcific deposits in the hip and knee joints [22] [23] [25] [26]. Currently, it is not clear how the abnormal type II collagen hetero-fibrils contribute to calcification in the joints as the cartilage was not analysed microscopically.

In the context of these reports, we provide here a case study describing how abnormal matrix proteins could be linked to calcification in hyaline cartilage via type II pro-collagen accumulation in chondrocytes and abnormal type II collagen hetero-fibrils in the ECM. Moreover, in relation to what has been described for intra-articular calcification in patients with OA, we provide additional background for an Endoplasmic Reticulum Storage Disease (ERSD) chondrocyte phenotype. This phenotype transforms into type X collagen-positive hypertrophic chondrocytes with MV release and a compromised ECM consisting of abnormal thick collagen fibrils and collagen bundles, which may in turn contribute to the calcification.

Finally, we discuss development of crystalline deposits in relation to collagen bundles and hole zones in thick abnormal type II collagen hetero-fibrils, to attempt to define the molecular mechanisms underlying this patient's condition.

## 2. Patient's History

The patient was a 27 years old woman of normal stature (height 173 cm, weight 80 kg) when referred to our clinic. She had, since early teenage years, participated in low level competition sport (handball), and over the years had had a few minor injuries to the knees. She could participate and perform as well as her team mates without problems until her late teenage years when she began to have pain in the right knee. She did not experience problems in other joints. No family members reported joint pain, orthopedic disorders or arthritis.

Arthroscopy with minor surgery was performed 3 times when she was 18 - 23 years with relief of symptoms. The surgical descriptions are not available.

At twenty-seven (27) years of age, she again had pain in the right knee and clinical signs of a meniscal lesion. She went to a private clinic for immediate treatment but no report of her treatment is available. In 2001, at age thirty (30) years, she fell and hurt her right knee. She had pain for 3 months and a further arthroscopy was performed. The cartilage on the patella and on the medial and lateral tibia plateau was grossly fibrillated. The menisci and ligaments were normal. Postoperatively the patient was not allowed to put weight on the right leg.

One month after the right knee was re-arthroscoped in the hope that a Steadmann procedure could be performed, the patella was found lateralized, and the cartilage on the lateral tibia plateau was degenerated to a degree that made it impossible to micro fracture the chondral lesions. Intra-articular crystals were seen. The patient was referred to the rheumatologic department where clinical examination showed no signs of arthritis of any kind.

Two months postoperatively the patient again experienced pain in the right

knee. After another 6 months, a MR-scan showed tendinitis of the intra-patellar ligament, and exercises for this were initiated which relieved some symptoms.

Two (2) years later, arthroscopy was again performed because of pronounced retro-patellar pain. Lateral release was performed. The cartilage had only slight fibrillation on the tibia plateau.

During the following year the patient continued to experience pain in the right knee. MR-scans showed a lesion of the medial meniscus. When she was 33, arthroscopy was performed. The menisci were normal, but again the tibia cartilage showed degeneration (*Outerbridge* 3). Crystals were noted in the cartilage on the tibia and femur, and 2 biopsies were taken with a curette from the hyaline cartilage on the medial femoral condyle; one from an area with crystals and one from a macroscopically unaffected cartilage surface. Analysis of these biopsies included histology and TEM, cell explant culturing and DNA analysis.

A synovial biopsy (data not shown) was obtained from the suprapatellar bursa and microscopic examination by a pathologist confirmed only unspecific inflammation.

When she was 36 years old arthroscopy was again performed. The findings were largely as previously noted. A medial plica was seen and resected, and a small (< 5 mm) lesion (*Outerbridge* 4) on the medial femoral condyle was microfractured. There is no report of the postoperative progress.

When she was 40 years old she had a distortion of the right knee and was seen in an outpatient clinic. There was no sign of any serious lesion, and the surgeon found no indication for arthroscopy. The patient requested a second opinion and went to a private clinic for an arthroscopy. The report is unavailable, but the procedure did not have a lasting effect. The symptoms from the right knee exacerbated in subsequent years, and she had a total knee prosthesis inserted in the right knee when she was 44 years old.

### 3. Material and Methods

#### 3.1. Tissue and Blood Analysis

Cartilage biopsies obtained from tissue adjacent to lesions in the tibia were supplied by Glostrup University Hospital (Denmark), following protocols reviewed and approved by an Ethical Committee (KA-05017-GM). Written, informed consent was obtained from the patient.

Tissue samples in calcium-free Dulbecco's Modified Eagle Medium (DMEM; InVitrogen) with added antibiotic (Gentamycin 49 ug/mL, Fungizone 1.2 ug/mL) and 87 ug/ml ascorbic acid 2-phosphate (Sigma Aldrich) were transferred to a cell laboratory in separate transport containers.

All tissue samples were rinsed in Tris/NaCl (Tris, NaCl Sigma Aldrich) under sterile conditions. The tissue samples were examined under an inverted light microscope (Nikon TMS-F, Japan) and 2 - 4 mm thick cartilage slices were cut from the cartilage biopsies by cutting perpendicularly towards the articular surface. These tissue slices represented all cartilage zones including calcified regions

in the upper to lower zone.

Cartilage slices were then immediately frozen in liquid nitrogen and stored for subsequent cryo-sectioning for light microscopy (LM) and immunohistochemistry. Other cartilage slices (not frozen) were used for explant culturing of chondrocytes (see below). Specimens for TEM were cut into 1 mm<sup>3</sup> pieces and immediately fixed in 2.5% Glutaraldehyde solution for 24 hours (see below).

### 3.2. Control Cartilage Biopsies

Biopsies from a male patient (age 39, height 180 cm) who received Autologous Chondrocyte Implantation (ACI) at the hospital, were used as control material. After trauma, he had developed a single chondral lesion (2 cm in diameter) on the medial femoral condyle. Several cartilage biopsies were obtained from a non-weight bearing area of the medial femoral condyle with healthy articular cartilage. The biopsies were obtained with a curette and divided between 2 transport containers with DMEM medium as described above. Container 1 was used for cell culturing in a GMP cell laboratory and later (3 - 4 weeks) used for the ACI procedure. Container 2 was treated essentially as described above (*Tissue and blood analysis* section) and cartilage pieces were analyzed by LM, TEM, Immunohistochemistry and explant culturing.

### 3.3. Pathological Studies Using Light Microscopy (LM)

The cartilage slices were removed from liquid nitrogen and mechanically fixed to a custom-built specimen holder. Sections 5 µm thick were cut on a cryostat (Leica CM 1850 Cryostat, Nussloch, Germany) and transferred to glass slides. The sections were fixed in 4% formalin buffered with Phosphate Buffered Saline (PBS) without calcium (InVitrogen) for 5 min and rinsed twice in PBS and distilled water, before staining with 1) 0.1% Toluidine Blue, (Sigma Aldrich); 2) 0.1% Hematoxylin and Eosin (H&E; Sigma Aldrich), and 3) 0.3% AgNO<sub>3</sub> for calcium (Von Kossa staining/Sigma Aldrich) and Safranin 0.1% (Sigma Aldrich). After de-staining in PBS (calcium free) or distilled water, the sections were mounted on glass slides with mounting media (Pertex art.no.00801, Histolab, Goteborg, Sweden). Both unstained and stained sections were examined under compensated polarized light and phase contrast microscopy (Leitz LaborLuxS and Nikon Eclipse TE2000-U microscopes, magnification; ×10, ×20). Images were obtained with a Nikon Coolpix 955 digital camera attached to the microscopes.

### 3.4. Immunohistochemistry

Immuno-histochemical studies of 5 µm cryo-sections were performed with a panel of mouse monoclonal antibodies against human 1) type I collagen (M1A34OM, Biodesign Int, USA, diluted 1/400); 2) type II collagen (II-4CII, MP Biomedicals, USA, diluted 1/200); 3) collagen VI (VI-26, ICN Biomedicals Inc, USA, diluted 1/200); 4) collagen X (COL-10, Sigma Aldrich, USA, diluted 1/400), and 5) aggrecan/keratin sulfates (1R11 14A6, BioSource, Belgium, diluted 1/200).

Cryo-sections were fixed 5 min in 4% formalin/PBS. Endogenous peroxidase activity was blocked with 0.3% hydrogen peroxide as per the vendor's protocol (ChemMate, DakoCytomation, Denmark). Before incubation with primary antibodies, sections were incubated in 10% normal goat serum/PBS (DakoCytomation) for 3 hours to block non-specific binding. Labeling was visualized with peroxidase using diaminobenzidine (DAB) as substrate. Avidin-biotin was used to enhance labeling of the monoclonal antibodies as per the manufacturer's instructions.

Negative control staining was performed by omitting primary antibody for both patient and control cartilage. Images of stained sections were recorded with a digital camera (see above). Following immunostaining for collagen type X, some sections were also co-stained with Von Kossa.

### 3.5. Explant Culturing.

Briefly, before explant culturing, cartilage biopsies were sorted into 2 groups and thereafter cut into smaller pieces; 1) explants with calcified islands, 2) explant without calcified islands (white-yellowish cartilage). Explants were transferred to separate 25 cm<sup>2</sup> cell culture flasks (InVitrogen) containing 10 ml growth medium. The growth medium comprised Dulbecco's Modified Eagle's Medium DMEM/NUT.MIX.F-12 medium with Glutamax-1 (InVitrogene), 15% Fetal Calf Serum (FCS) (InVitrogen), Gentamycin (49 ug/ml) and Fungizone (1.2 ug/ml) (all reagents, Sigma Aldrich). Explants were cultured for 3 weeks with fresh medium added every third day. During the culture period, images of chondrocyte outgrowth from explants were obtained with a Nikon Coolpix 955 digital camera attached to an inverted light microscope (Nikon TMS, 10×, 20×).

Explant cultured chondrocytes for further analysis were harvested from the culture flasks by physical removal of cells with a cell strainer.

Control cartilage explants were treated essentially as described above, sorted into a single group.

### 3.6. Transmission Electron Microscopy (TEM)

Cartilage biopsy samples including control samples, and approx.  $1.0 \times 10^6$  explant cultured chondrocytes/culture flask were processed for TEM.

Briefly, glutaraldehyde-fixed cartilage sections and explant cultured chondrocytes were first fixed in 2% osmium tetroxide for 1 hour and samples were thereafter embedded in Epon resin. One-micron (1 μm) sections were stained with 0.1% Toluidine Blue (Sigma Aldrich) for orientation.

Subsequently, ultra-thin sections cut on a microtome, were mounted on 150-mesh copper grids and stained with uranyl acetate/lead citrate before TEM examination (Phillips EM208, Philips; Eindhoven, The Netherlands). Upper-lower cartilage zones and cell aggregates from explant culturing were analyzed. Condensed collagen bundles, calcified bodies/islands, matrix vesicles (MV) and hypertrophic chondrocytes in the patient's cartilage were particularly investigated.

Measurements of collagen fibril diameters in cartilage and within calcified islands were carried out with Mega view III soft imaging system (Münster, Germany). Both collagen fibrils in longitudinal sections and fibrils in a cross-sectional view were measured. Mean diameters of fibrils and Standard Deviation (SD) of the mean were indicated.

### 3.7. Molecular Studies

Genomic DNA was isolated from explant cultured chondrocytes. Approximately  $1.0 \times 10^6$  chondrocytes were used for genomic DNA isolation as per a protocol developed by the manufacturer (Wizard Genomic, Promega, Madison WI, USA).

Primers were synthesized by TAGC-Copenhagen (Copenhagen, Denmark) and designed based on published sequences for the entire human *COL2A1* gene sequence (accession number L10347; GenBank/EMBL database), for subsequent analysis by Polymerase Chain Reaction (PCR). Primer pairs were designed to conform to conventional rules for primer selection. Approximately 100 ng of DNA/25 $\mu$ l reaction mixture was used for PCR amplification.

All 54 exons including flanking intronic sequences (approx. 10 - 20 base pairs) and some intronic sequences between adjacent exons of the *COL2A1* (27) gene were amplified by PCR and 20% of the PCR product was analyzed by electrophoresis in 1% agarose. The remaining PCR products were purified on a mini spin column according to the manufacturers' instructions (Wizard PCR clean up system, Promega, Madison WI, USA). The purified DNA fragments, together with both sense and anti-sense sequencing primers were sent to GATC-Biotech AG (Konstanz, Germany), for bi-directionally sequencing.

Molecular analysis was not performed on the control cartilage.

## 4. Results

### 4.1. X-Ray

Radiographs of the patient's right knee joint (**Figure 1**) demonstrated calcifications in both menisci and in the cartilage of the lateral compartment. On the lateral margin of the medial femoral condyle a small osteophyte was visible and there was a slight flattening of the medial femoral condyle indicating a very early degenerative condition (**Figure 1**, radiograph of the patient's knee joint at age 35).

Radiography of the control patients' knee joint was normal and demonstrated no sign of calcification in menisci and cartilage (data not shown).

### 4.2. LM of Cartilage

Macroscopically, the articular cartilage biopsy samples were distinctly colored with white-yellowish tissue containing darker, intra-articular poly-amorphous bodies (**Figure 2**). This pattern was present in the upper to lower zones and areas of calcification could be seen as regions within these bodies (**Figures 2(A)-(D)**). The

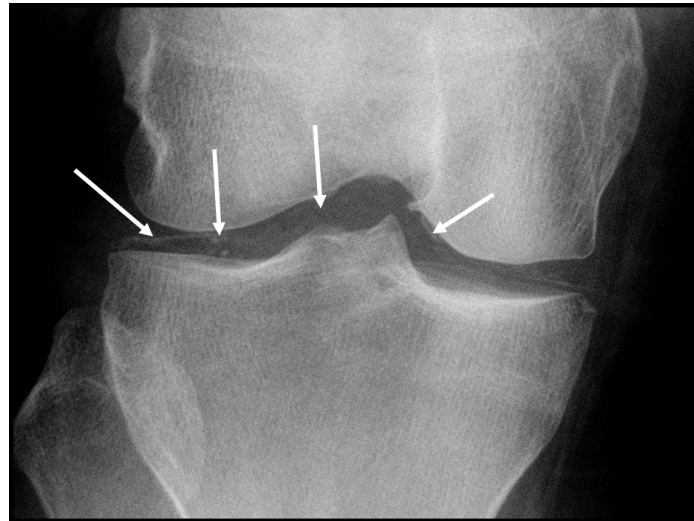


**Figure 1.** An X-ray of the patient's right knee joint (age 35). On the lateral side of the medial condyle, small osteophytes are visible. Note calcification in both menisci and on the articular cartilage (lateral compartment, white arrows) which is typical of chondrocalcinosis.

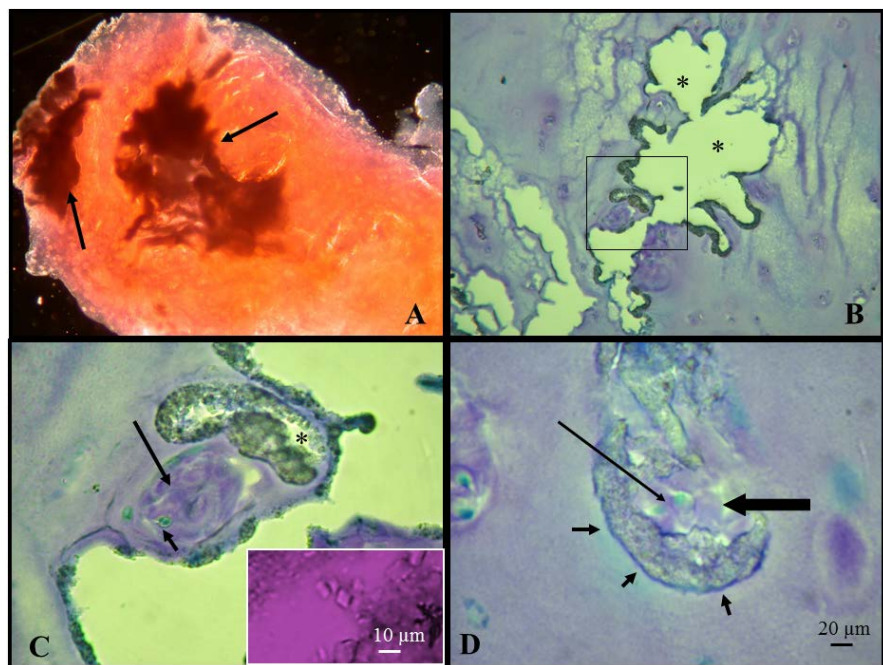


**Figure 2.** (A) Shows a section (mag 4 $\times$ ) of cartilage biopsy stained with Safranin O. Calcified islands (arrows) are evident. (B) Calcified matrix was lost (\*) during sectioning, creating holes in the cartilage. Fibrocartilage is present adjacent to the calcified matrix in the Toluidine Blue stained section (mag 10 $\times$ ). Higher magnification of the matrix marked in the square is shown in (C) (mag 20 $\times$ ) where rod and rhomboid-shaped CPPD crystals in lacunae (\*) are visible. Collagen bundles (long arrow) are also seen adjacent to chondrocytes (short arrow; see also TEM **Figure 8(A)** & **Figure 8(B)**). The inserted micrograph in (C) shows rhomboid CPPD crystals under compensated polarized light (unstained section). (D) shows a calcified matrix zone (short arrows) progressing in close proximity to cartilage cells (long thin arrow) suggesting that chondrocytes are directly involved in calcification (mag 20 $\times$ ).

amorphous bodies will hereafter be named calcified islands.

Under compensated polarized light, weakly birefringent and rhomboid or rod-shaped calcium pyrophosphate dehydrate (CPPD) crystals with diameters of 5 - 10  $\mu\text{m}$  were observed (**Figure 2(C)**, see smaller inserted picture). These crystals were identified in the chondrocyte's peri-cellular compartments, adjacent to collagen bundles (**Figure 2(D)**). In addition, deposition of amorphous non-birefringent clumps of crystal structures (radial clusters of needle-like crystals) resembling Hydroxyapatite-like crystals was also identified within the calcified islands. Further identification and characterization of these amorphous clumps/crystal rosettes, was performed with TEM as described below (see section for TEM—ultrastructural characterization).

Poorly differentiated and occasionally bizarre spindle-shaped chondrocytes were identified in a mixture of fibro- and hyaline-cartilage. In addition, the matrix showed weak staining with Toluidine Blue indicative of a reduction of matrix components (**Figure 2(B)**).

### 4.3. Immunohistochemistry

Strong staining for collagen type II collagen (**Figure 3(A)**) and aggrecan (data not shown) was especially observed within the calcified islands and particularly within the chondrocytes (**Figure 3(B)**). Staining of chondrocytes was more intense in comparison to the ECM suggesting intracellular deposition of type II pro-collagen components. It was noteworthy that where the ECM showed calcification, there was intense staining for collagen type X (**Figure 3(C)**, **Figure 3(D)**), a marker for chondrocyte hypertrophy. Non-calcified cartilage (white-yellowish) areas remained unstained for this marker. Some staining for collagen type I were also noticed within the calcified islands and fibrocartilage while type VI collagen was closely associated with the chondrocytes surface. Some staining was also noticed in the territorial cartilage matrix (data not shown).

Tissues which were positive for collagen type X also stained positive with von Kossa stain, confirming that type X collagen was associated with calcification (**Figure 3(D)**).

### 4.4. LM of Explant Cultured Chondrocytes

To attempt to answer the questions of whether matrix accumulation was an intrinsic function of chondrocytes from both tissue areas and whether matrix accumulation in chondrocytes was linked to calcification, LM was performed on isolated explants with (**Figure 4(A)**) or without calcified islands (small inserted micrograph in **Figure 4(B)**).

Observation of outgrowths of chondrocytes derived from explants [28] with numerous calcified islands (**Figure 4(A)**) showed they contained large intracellular inclusion bodies (**Figure 4(B)**). This was interpreted as matrix accumulation, a suggestion supported by TEM (see below under TEM section) which definitively demonstrated that matrix accumulation was indeed present in dilated rER (**Figure 4(C)**, **Figure 4(D)**). During further culturing of chondrocytes with inclusion

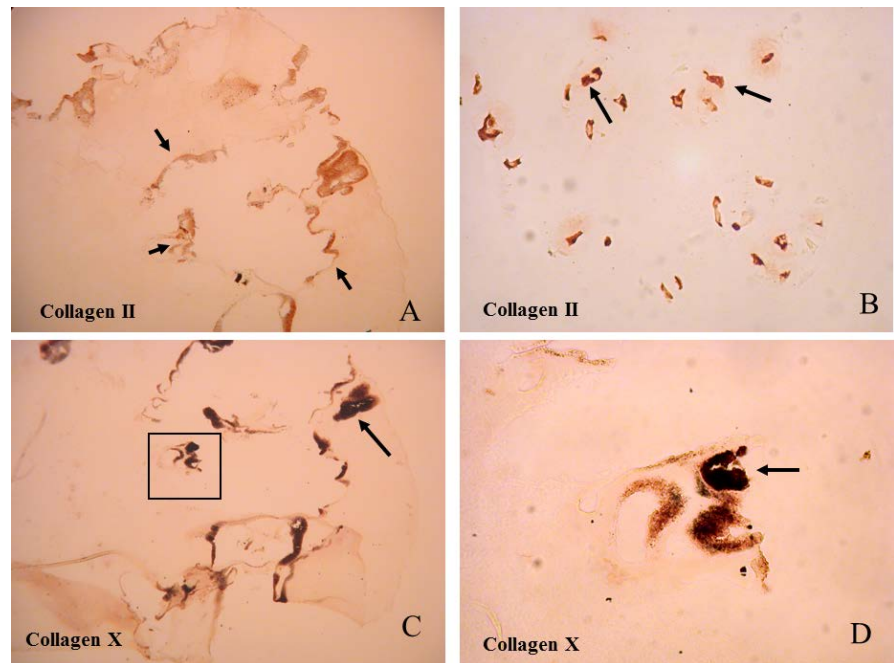


**Figure 3.** Shows immuno-stained cartilage sections. (A) shows a section with calcified islands (short arrow), stained with anti-collagen II antibodies. Strong staining of Collagen II is especially seen within the calcified islands (short arrows) but staining is also present throughout the non-calcified matrix. Note again, that loss of calcified matrix during sectioning leave artificial holes in the cartilage (mag 4×). (B) shows a section stained with anti-collagen II antibodies. Strong intracellular staining in chondrocytes (arrows) is evident indicating that pro-collagen type II is accumulated within the organelles (mag 20×). (C) shows a section stained with anti-collagen X antibodies (brown precipitate), and co-stained with von Kossa (black precipitate indicated with an arrow). Strong staining within the calcified islands is evident. **Figure 4(D)** shows a higher magnification (mag ×40) of the calcified areas in (C) (square). Co-staining with anti-collagen X antibodies and Von Kossa (indicated with an arrow) staining demonstrates that calcification is linked to expression of type X collagen by hypertrophic chondrocytes.

bodies, several cells turned into floating dead “ghost cells” (data not shown). In comparison, chondrocytes derived from non-calcified explants did not express inclusion bodies. These results suggest that chronic ER stress and matrix accumulation in chondrocytes could somehow be linked to the calcified islands in the cartilage. In addition, it was also speculated that a threshold level (probably high) of matrix accumulation is needed for the transformation of chondrocytes into hypertrophic cells and subsequent calcification (see discussion).

Chondrocyte outgrowth from control explants showed no evidence of inclusion bodies/matrix accumulation within the cells’ cytoplasm. This finding was confirmed early in the culture period (1 - 2 weeks, **Figure 4(B)** + inserted micrograph) and after 3 - 4 weeks of culturing (data not shown).

#### 4.5. TEM-Ultrastructural Characterization

The upper-middle cartilage zones were selected for ultra-structural studies.

Chondrocytes within the calcified islands appeared highly atypical and showed a

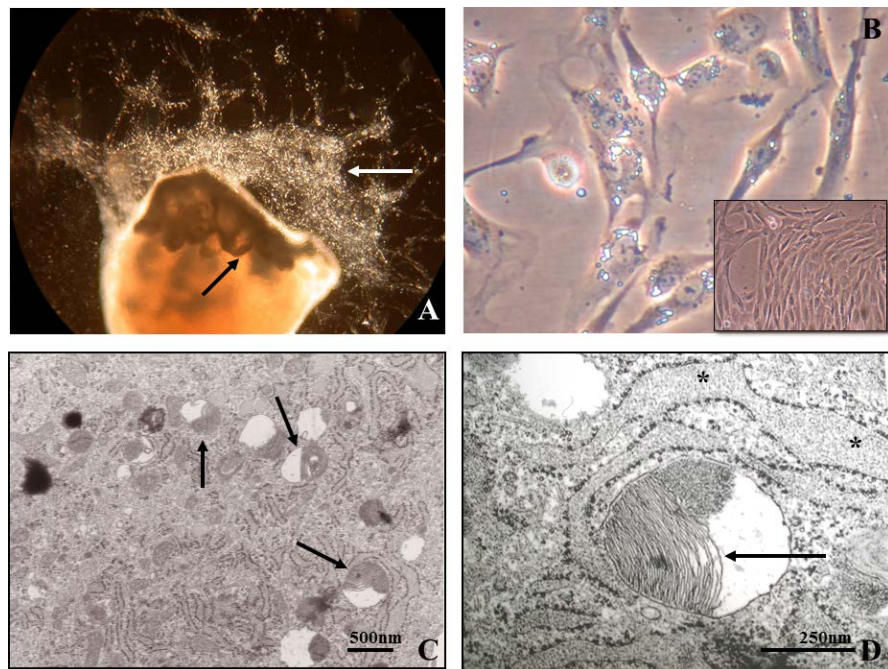


**Figure 4.** (A) is a light micrograph (mag 4×) of a cartilage explant cultured for 1 - 2 weeks. Chondrocyte outgrowth (white arrow) from calcified islands (black arrow) is evident. (B) shows chondrocyte outgrowth at higher magnification (mag 20×) from calcified areas of an explant. Intracellular matrix accumulation indicates that matrix accumulation is linked to calcification. The inserted micrograph shows explant derived chondrocytes isolated from normal cartilage (mag 10×). (C) is a TEM of explant derived chondrocytes from calcified islands (mag ×5.2K), revealing intracellular matrix accumulation of collagen fibrils (arrows). (D) is a higher magnification (mag ×20K) TEM of matrix accumulation in rER (\*) with pro-collagen filaments stacked in parallel (arrow).

highly disorganized cytoplasm containing numerous secretory vesicles dispersed throughout the cytoplasm. In addition, chondrocytes showed a remarkably enlarged and distended rER formation (**Figure 5(A)**, **Figure 5(B)**) which was in close association with distended Golgi cisterna. It was evident that there was accumulation of matrix proteins in rER, showing filamentous ultra-structures with diameters of 1 - 2 nm (**Figure 5(B)**) which were also seen in explant cultured chondrocytes (**Figure 4(C)**, **Figure 4(D)**). In comparison, chondrocytes in the non-calcified cartilage (white-yellowish) also showed matrix accumulation but the cell morphology and cytoskeleton were less affected (compare **Figure 5(A)** and **Figure 5(C)**). Apoptotic chondrocytes with intracellular accumulation of collagen like filaments and fibrils were also detected in the calcified islands (**Figure 5(D)**) as well as “outside” these bodies.

The ECM was dominated with abnormally thick collagen hetero-fibrils of abnormal appearance, with diameters in excess of 100 nm. The matrix also showed electron-dense amorphous material including proteoglycans and debris of cellular components, and there was a reduction in the formation of type II collagen hetero-fibrils (**Figure 5(A)**, **Figure 5(B)** and **Figure 6(C)**, **Figure 6(D)**).

In addition, large bundles of parallel-oriented thick type II collagen hetero-

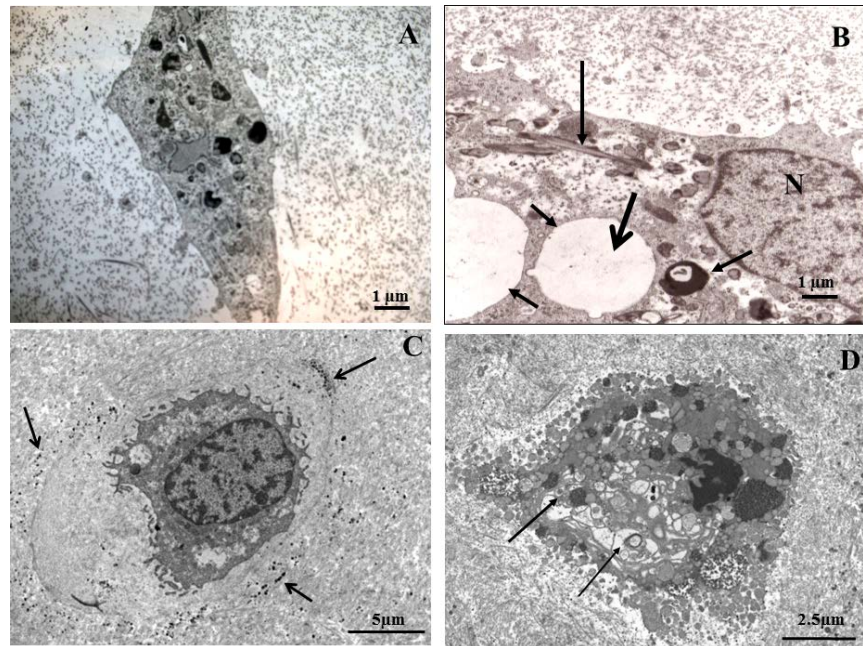


**Figure 5.** Shows TEMs of hypertrophic chondrocytes in the calcified matrix. (A) shows a highly atypical chondrocyte with matrix accumulation in distended rER as well as within other organelles (mag  $\times 4K$ ). (B) shows a chondrocyte containing intracellular collagen fibrils (long arrow) and accumulation of matrix proteins in vesicles (short arrows). N indicates the nucleolus. The thick arrow shows areas where matrix was lost during sectioning (mag  $\times 4K$ ) (C) shows another hypertrophic chondrocyte with matrix vesicles (arrows) in the pericellular compartment (mag  $\times 1.6K$ ). (D) shows an apoptotic chondrocyte with intracellular accumulation of collagen-like filaments and fibrils (indicated with 2 arrows) (mag  $\times 1.6K$ ).

fibrils were identified in the ECM (**Figure 6(A)**, **Figure 6(B)**). Numerous collagen fibrils in the bundles had diameters larger than 100 nm which is unusual in mature articular cartilage: the diameters of collagen fibrils in control cartilage were  $52 \text{ nm} \pm 19 \text{ nm SD}$ . Further, electron-dense materials were seen within the collagen bundles indicating protein aggregates and some calcification of matrix proteins. Short (truncated) and abnormal forms of collagen fibrils were also seen in the calcified ECM (**Figure 6(C)**) as well as “outside” the calcified islands (**Figure 6(D)**) indicating that all chondrocytes synthesize abnormal protein.

**Matrix Vesicles (MV)** with a double layer membrane and with diameters of 100 - 200 nm, (mean  $169 \pm 57 \text{ nm}$ ) were identified (**Figure 7(A)**, **Figure 7(C)**, **Figure 7(D)**) in the (hypertrophic) chondrocytes’ peri-cellular matrix compartment, consistent with MVs reported in humans [29]. Matrix vesicles were often seen associated with individual needle-like hydroxyapatite crystals in the peri-vesicular area (**Figure 8(B)**). Both intact MVs (**Figure 7(C)**, **Figure 7(D)**) and MVs in which crystals had outgrown the vesicles (**Figure 8(B)**) were observed. Numerous MVs also showed association with type II collagen fibrils of various diameters (100 - 200 nm) (**Figure 7(C)**, **Figure 7(D)**). In particular, HA like crystals in the form of clumps/rosettes were seen adjacent to collagen fibrils or inside these fibrils suggesting that abnormal collagen fibrils might be involved in

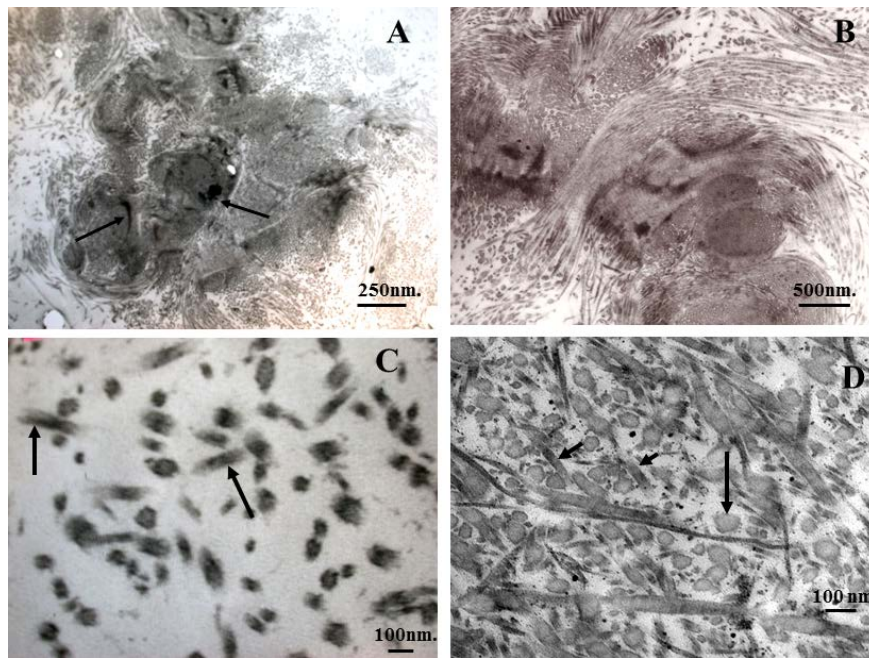


**Figure 6.** (A) and (B) are TEMs showing unusual compartments within the calcified islands, which contain giant bundles of thick collagen hetero-fibrils. Neither MVs nor calcified areas were not identified within the bundles suggesting that bundles do not contribute to calcification (mag  $\times 5K$  and  $10K$ ). (C) shows highly abnormal truncated (arrow) collagen fibrils seen at the periphery of the collagen bundles (mag  $\times 30K$ ). (D) shows these abnormal truncated collagen fibrils (small arrows) are also observed outside the calcified islands. Some fibrils have diameters of nearly 100 nm (long arrow) (mag  $\times 30K$ ).

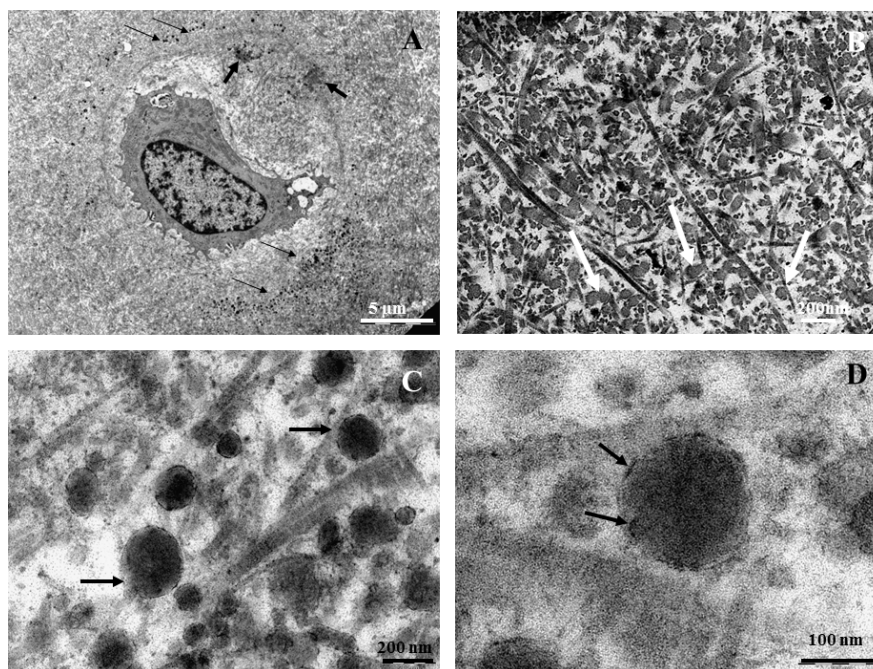


**Figure 7.** Shows TEMs of hypertrophic chondrocyte. (A) shows a hypertrophic chondrocyte with numerous matrix vesicles in the pericellular compartment (thin arrows). Calcified matrix is also evident (thick arrows, mag  $\times 1.6K$ ). (B) is a higher magnification (mag  $\times 20K$ ) TEM of the interterritorial compartment in (A). Abnormal thick truncated collagen fibrils (arrows) are very prevalent in the ECM. (C) further highlights matrix vesicles (arrows) identified in (A). Numerous vesicles (arrows) are seen adjacent to type II collagen heterofibrils (mag  $\times 30K$ ). (D) shows needle-like electron dense crystalline apatite mineral precipitate (arrows) within matrix vesicles (mag  $\times 96K$ ).

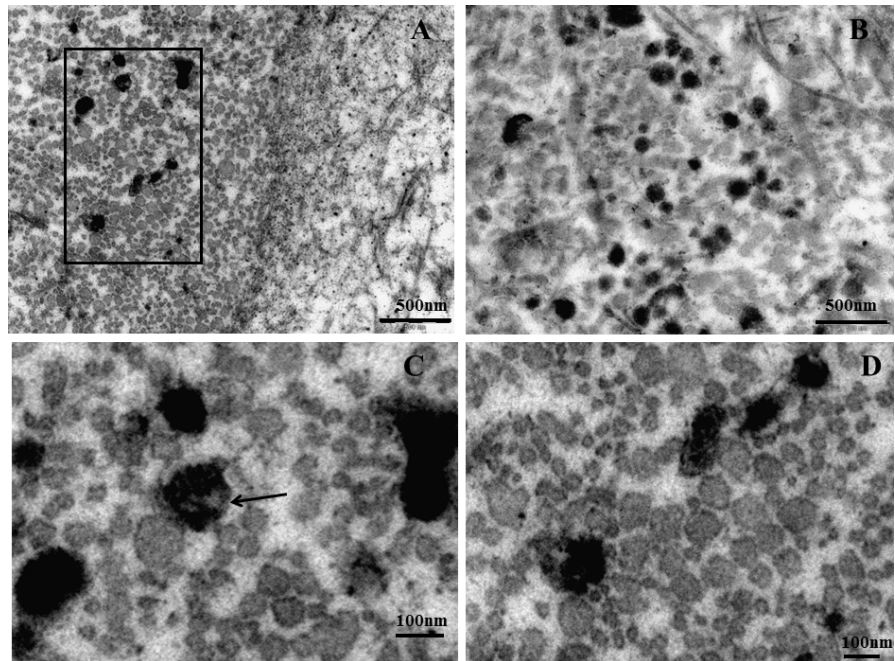


**Figure 8.** Shows TEMs of calcifying areas in the cartilage matrix. (A) shows crystalline apatite mineral within thick collagen fibrils, with diameters up to 100nm (mag  $\times 16K$ ). (B) shows putative ruptured matrix vesicles with apatite crystals in clumps or globules, again adjacent to collagen fibrils (mag  $\times 16K$ ). (C) and (D) are higher magnifications (mag  $\times 40K$ ) of the highlighted area from (A). These micrographs demonstrate that hydroxyapatite like crystals can develop on the surface and within (arrow) the collagen fibrils. Both thin and thick collagen fibrils seem to mediate crystal growth.

the initial phases (nucleation) of calcification. These crystalline clumps/rosettes had similar diameters to the diameters of the collagen fibrils (100 - 200 nm) with which they were associated (**Figures 8(A)-(D)**).

#### 4.6. Control Cartilage Examined by TEM and LM

TEM of control cartilage (**Figure 9(C)**, **Figure 9(D)**) showed normal chondrocytes in an organized ECM with normal type II collagen hetero-fibrils (diameter  $52 \text{ nm} \pm 19 \text{ nm SD}$ ,  $n = 42$ , measured within the inter-territorial compartment). Secretory vesicles in the chondrocytes had normal sizes and rER showed no evidence of matrix accumulation (**Figure 9(C)**). Absence of apoptotic chondrocytes was also confirmed.

Some matrix like-vesicles were detected in the control biopsies (**Figure 9(C)**, arrow) but they were few in number compared to the patient with calcification in the cartilage (compare **Figure 5** with **Figure 9(C)**). Further, there was no evidence of crystals or calcification within the ECM or close to matrix like-vesicles.

LM of control cartilage (before staining) showed macroscopically white-yellowish tissue (data not shown) with absence of darker, intra-articular bodies as shown in **Figure 2**.

Staining with Toluidine Blue (**Figure 9(A)**) confirmed a homogenous stained ECM in which the upper to lower cartilage zones were without calcification. No

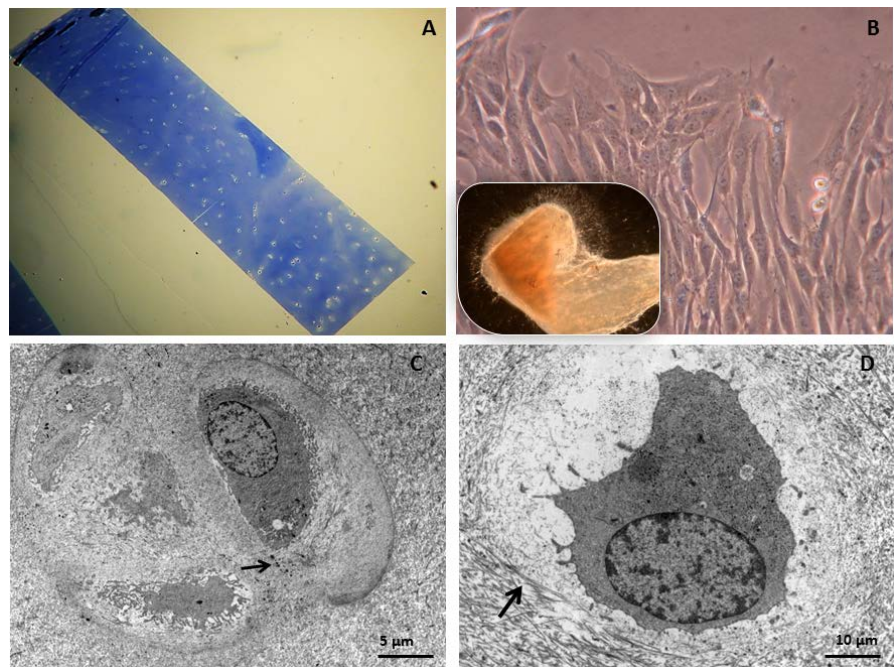


**Figure 9.** Control cartilage; (A) Toluidine Blue stained cartilage, (B) Cartilage explant cultured chondrocytes (inserted micrograph shows cell out-growth from explant) unstained, (C)-(D) TEM of control cartilage. Arrows in (C) and (D) point to matrix like-vesicles and type II collagen hetero-fibrils, respectively.

collagen bundles were present (**Figure 9(A)**).

Control cartilage examined by LM and immunochemistry (**Figure 10**) showed negative staining for collagen type I (A) and collagen type X (D), strong positive staining for aggrecan (C) and medium positive staining for collagen type II (B). Collagen type II showed strong peri-cellular staining (B, arrow) together with Type VI collagen (data not shown).

#### 4.7. Explant Cultured Chondrocytes

There was no evidence that chondrocytes derived from explants with calcified islands exhibited intracellular calcification. In contrast, these atypical chondrocytes showed a remarkable accumulation of matrix proteins within distended rER and Golgi cisternae as well as numerous irregularly shaped secretory vesicles contained in large cytoplasmic vacuoles, which influenced the overall chondrocyte morphology (**Figure 4(C)**, **Figure 4(D)**).

Chondrocytes isolated from the non-calcified white-yellowish cartilage explants also showed accumulation of matrix proteins in rER and Golgi cisternae. “Tread like” ultra-structures resembling filaments within distended rER were also identified in these organelles (data not shown).

Extracellular matrix proteins synthesized by cultured chondrocytes also showed collagen fibrils of poor quality indicating that chondrocytes in vitro also synthesised abnormal protein.

Chondrocytes derived from control explants showed normal cell morphology

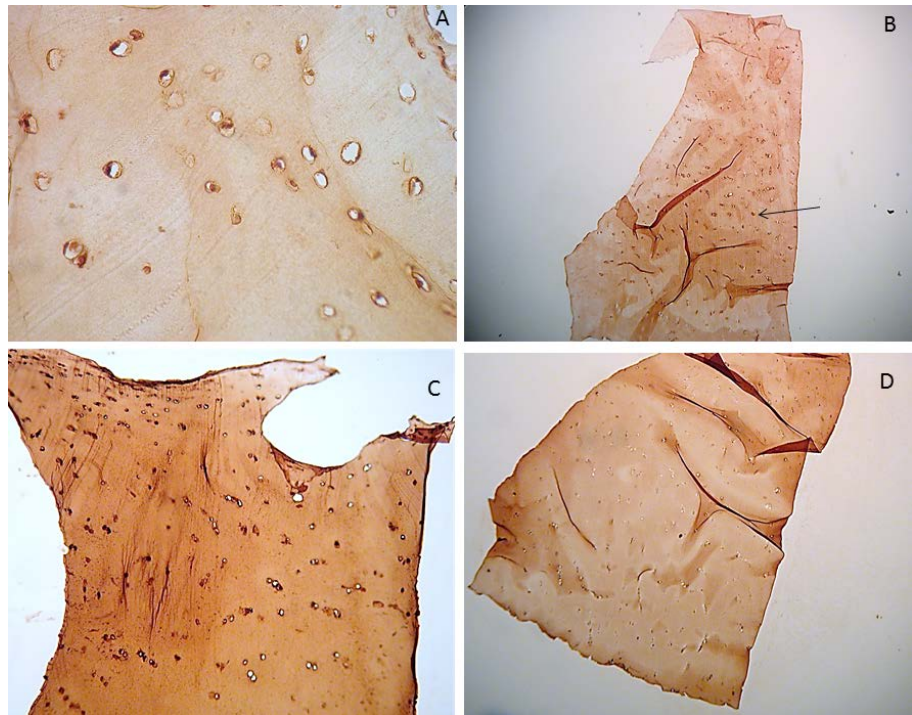


**Figure 10.** Immunohistochemistry of control cartilage with; (A) anti-collagen type I Abs, (B) anti-collagen type II Abs, (C) anti-aggrecan Abs, and (D) anti-collagen X Abs. Arrow in picture B indicate a strong peri-cellular staining.

with some evidence of a fibroblastic phenotype. There was no formation of intra-cellular crystals or matrix accumulation (data not shown).

#### 4.8. Molecular Analysis

All 54 exons and some introns of the *COL2A1* gene were sequenced to determine if anomalies in type II collagen hetero-fibrils were caused by DNA mutation. However, no mutations were found in the *COL2A1* gene. Only single nucleotide polymorphisms (SNP) were found: T9S (A > T) in exon 1, G612G (T > TC) in exon 28 and V1331I (G > GA) in exon 52.

### 5. Discussion

In this case report, we observe that, in contrast to control cartilage, articular cartilage biopsies from a patient with calcification in one knee joint, display a complex pattern of 1) chondrocytes with accumulation of type II pro-collagen in dilated rER, and 2) calcified ECM containing collagen bundles and abnormally wide type II collagen-fibrils. In addition, a current paradigm for this chondrodysplasia-like phenotype with intra-articular calcification suggests that the phenotype might be a result of matrix accumulation which transforms cartilage cells into active type X collagen secreting hypertrophic chondrocytes, which release MV into the ECM, and initiate crystal formation and deposition together with thick abnormal collagen fibrils leading to a highly compromised ECM.

Several phenotypic changes described for this patient's chondrocytes and

ECM, also demonstrated with explant cultured chondrocytes from the patient, are similar to findings in certain human type II collagenopathies [30] [31] such as Stickler syndrome, Kniest dysplasia and spondyloepiphyseal dysplasia (SED) [30]. These include matrix accumulation in rER in chondrocytes [32], abnormal type II collagen hetero-fibrils composed of fibrils with increased fibril diameters, collagen bundles in the ECM of the cartilage [30] and cell death [33]. These features have also been shown to be present in cartilage from patients with juvenile Osteo Chondritis Dissecans (OCD) [27] and in patients with patellofemoral dysplasia involving patella alta and trochlea dysplasia [28].

The ultra-structural characterization of filaments with a lamellar appearance and a diameter of 1 - 2 nm accumulated in rER, has to our knowledge not been reported before. Since fibrillar collagen molecules are derived from pro-collagen triple-helix formation in the rER with a length of 300 nm and diameters of 1.5 nm [34], and immuno-staining confirmed that type II collagen had accumulated in chondrocytes, this suggests that accumulated filaments (**Figure 4(C)**, **Figure 4(D)**) might be identical to retained self-assembled triple-helical type II pro-collagen chains. These findings may indicate that pro-peptides do not prevent intracellular fibril formation in rER, since released triple-helical collagen monomers have an intrinsic property for self-assembly into fibrils. This in turn suggests that pro-peptides are either removed before secretion or contain a dysfunction in the globular extensions at the N- or C-terminal ends.

Neither filaments nor accumulation of other matrix proteins in rER were identified in chondrocytes derived from control cartilage.

In relation to dysfunctional type II pro-collagen molecules in osteochondrodysplasia including Stickler and Kniest syndromes, a mutation in the *COL2A1* gene has been associated with calcium deposition diseases. A point mutation (A75C) in the *COL2A1* gene has been identified in 4 families in 4 different countries (Chiloe Island, France, United States and Finland), associated with tall stature, hearing loss and early-onset OA. In 3 out of the 4 families the mutation was also associated with cartilage calcifications which include CPPD and HA crystalline deposits [22] [23] [25] [26]. In comparison with the more than 100 different *COL2A1* mutations which have been assigned and listed in the Human Gene Mutation Database (HGMD) at <http://www.hgmd.org>, the A75C mutation is the only mutation in the *COL2A1* gene which has so far been associated with CPPD and HA deposition. However, these studies did not report any morphological examinations of chondrocytes or calcified cartilage and a comparison with our findings is therefore not possible. Also at a molecular level, since DNA sequencing of the *COL2A1* gene for this patient only revealed single nucleotide polymorphisms (SNP) within the 54 exons examined, no disease-causing mutation could be linked to this patient's phenotype, although it cannot be ruled out that the absence of identifying a disease-causing mutation(s) in the *COL2A1* gene could be the result of a technical shortfall. In addition, other possibilities for the presence of abnormal type II collagen hetero-fibrils might relate to sequence alterations that exist in different genes in different loci. For instance,

screening for mutations in the *COL9A1*, *COL9A2*, *COL9A3*, *COL11A1*, and *COL11A2* genes, which code for type IX and type XI collagens, might be revealing as these collagens form hetero-fibrils with type II collagen. Mutations in any of these genes could theoretically give rise to abnormalities in type II collagen hetero-fibrils which could lead to fibril accumulation in rER and abnormal type II collagen hetero-fibrils.

Abnormal pro-collagen synthesis and intracellular pro-collagen accumulation could have an impact on cell differentiation, but how is difficult to address as the highly abnormal ER-stressed compartments might exert direct effects on the cells' behaviour. For instance, type II collagen has been reported to be required for chondrocyte survival [35] and synthesis of collagen type II is down-regulated with chondrocyte hypertrophy, the stage where synthesis of the non-fibrillar collagen type X is initiated [36]. This suggests that "blocking" of type II collagen synthesis because of accumulation in rER could lead to chondrocyte hypertrophy or cell death [28], or both. The proposed pathways might be controlled by the extent of matrix accumulation.

There is still some controversy about where nucleation occurs for calcification and the exact molecular nature of the initiator(s) of nucleation. Some groups propose that MVs are the sites of initial nucleation [37] [38] but the exact mechanisms through which MVs orchestrate the calcification process remain unclear. Common proteins identified in relation to MVs and calcification (recently reviewed by Cui L *et al.*, [39]) are; phosphate transporters, calcium binding proteins (Annexins), cell surface proteins (Integrins), extra cellular proteins (collagen type I, IV, proteoglycans), phospholipids and chaperons (Calreticulin) [40] [41] [42] [43] [44].

Matrix Vesicles which arise from hypertrophic chondrocytes by a budding process [45] [46] [47] were clearly present in areas of calcification in this patient's biopsies. In addition, as shown by immunostaining for type X collagen which is a collagen marker for chondrocyte hypertrophy and calcification [1], there was a strong anti-type X collagen staining within the calcified islands without any histological evidence of staining within non-calcified cartilage (plain white-yellowish cartilage), suggesting that hypertrophic chondrocytes themselves may play an active role in crystal formation by producing and releasing MVs into the ECM. This further suggests that type X positive hypertrophic chondrocytes could induce and control the degree of earliest calcification in the territorial matrix compartments while maintaining the peri-cellular compartments mineral free. This tissue distribution posits a hypothesis that a unique combination of certain ECM components may be necessary for crystal formation and that hypertrophic chondrocytes may initiate the formation of these crystals. In the same context, chondrocytes derived from the cartilage explants with numerous calcified islands exhibited severe matrix accumulation with large inclusion bodies in the cultured cells (Figure 4(B)). In comparison, chondrocytes derived from explants with absence of calcified islands, showed a lower level of matrix accumulation (compare Figure 4(B) with inserted micrograph in the

same picture) with inclusion bodies not visible by LM even though matrix accumulation was evident by TEM. These findings suggest that collagen type II positive chondrocytes in plain cartilage might be in transition, before they undergo hypertrophy and express collagen type X, as a result of high protein accumulation.

The occurrence of thick abnormal type II collagen fibrils (average diameter > 100 nm) associated with MVs (**Figure 7(C)**, **Figure 7(D)**), compared to control cartilage with thinner, normal fibrils with an average diameter of 52 nm, might somehow be a factor which can induce and facilitate crystal growth after putative rupture of the MV membrane as shown in **Figure 8(B)**; for this, we hypothesize 2 mechanisms of how crystal development could propagate in the ECM.

One possible mechanism derives from the observation that intact MVs contained hydroxyapatite-like crystals suggesting that vesicles may be the site of primary nucleation. A second possible mechanism derives from the observation that the hydroxyapatite-like crystals were highly associated with thick abnormal type II collagen fibrils (**Figure 7** and **Figure 8**). Indeed, there was some evidence that crystals were formed on the inside of the collagen fibrils (**Figure 8(C)**) indicating that abnormal collagen fibrils themselves could direct nucleation and that a specific matrix environment is required for calcification to occur. In this context, both normal type I and type II collagen fibrils have been shown to act as scaffolding along which the hydroxyapatite crystals can grow [27] [37] [48]. Further, study models by Tong *et al.* [49] have shown that small hydroxyapatite platelets (with sizes of approximately 9 nm × 6 nm × 2 nm) can fit into aligned hole zones in the fibrillar collagen structure as postulated by Tong *et al.* [49]. They suggested from their studies that small hydroxyapatite crystals can enter the fibrils, probably via the hole-zones and fibrillar pores/intra-fibrillar collagen space, and that they can further propagate in the fibrils to fill all space. In comparison to the thick abnormal type II collagen hetero-fibrils described in this patient's samples, hole-zones with a changed (larger?) diameter might indeed be present in these fibrils and could therefore act as a scaffold where hydroxyapatite can grow.

For this case study dealing with prominent pathological calcification in the articular cartilage and meniscus, in contrast to the absence of crystals and calcification in control cartilage, the differentiation of BCP (e.g., hydroxyapatite) and CPDD crystals is an important consideration as there are differences between these crystals with respect to their clinical patterns and their aetiologies [50]. However, for differentiation of hydroxyapatite crystals, chemical analysis for molecular identification was not employed but TEM was used and demonstrated that hydroxyapatite-like crystals were formed adjacent to type X collagen positive hypertrophic chondrocytes and especially in the areas where MVs and thick abnormal type II collagen hetero-fibrils were concentrated. With regard to CPPD crystals (which were identified based on a rhomboidal/rod shaped birefringent crystal morphology with a diameter of 1 - 20 µm), relatively little is known about the role of the ECM composition and how individual proteins play

a role in CPPD crystal formation and growth. For instance, CPPD crystals are relatively unique to hyaline and fibro-cartilage but have also been found in OA [1] and within sites of chondroid metaplasia [51]. It has been reported [52] that the earliest CPPD crystals occur in the peri-cellular matrix/space surrounding articular chondrocytes. This is different from this case report where CPPD crystals were found in both the territorial as well as the inter-territorial matrix compartments suggesting that chondrocytes were not directly associated with the site of crystal formation. This suggests that CPPD crystal formation is not initiated at the same sites as MVs are released by hypertrophic chondrocytes. The finding could indicate that CPPD crystals are formed after hydroxyapatite like crystal development.

A final comment worthy of note in a discussion of crystal nucleation, relates to Chondrocalcin, a calcium-binding protein with strong affinity for hydroxyapatite. C-propeptide, once cleaved from type II collagen molecule (known as Chondrocalcin), has been reported to be associated with cartilage calcification in both healthy and diseased tissue [53]. It is relevant to speculate about the possibility that this peptide could also play a role in crystal assembly and calcification, even when still attached to the collagen molecule (e.g., cleavage of the C-propeptide could be blocked because of changes in secondary and tertiary collagen structure). For instance, where high local concentrations of abnormal collagen molecules/collagen aggregates are present, the C-propeptide could act as a nucleating agent for apatite formation. This is of course speculation but the hypothesis could be tested on calcified cartilage from OA patients and patients with collagen diseases [22] [23] [25] [26].

Further studies are needed to establish the complete chemical identification of the 2 different crystal forms reported in the cartilage, the origin and mechanism of CPPD crystal development and to determine whether they originate in the cartilage itself, or from hypertrophic chondrocytes, or from lymphatic drainage, or by some other mechanism (metabolic disease, familial, post-traumatic injury). In addition, studies investigating abnormal heterofibrils and ER procollagen accumulation in OA cartilage of older individuals, with or without calcium deposit, are needed as the current literature in this field is very limited.

## 6. Conclusions

In summary, the changes in articular cartilage reported for this patient were primarily related to accumulation of dysfunctional pro-collagen in chondrocytes and abnormal collagen fibrils in the ECM, and a femoral condyle with a chondrodysplasia like cartilage phenotype with intra-articular calcification. Further, it was suggested that type II pro-collagen accumulation starting in rER and later affecting other cell organelles induced chondrocytes, undergo hypertrophy and initiate calcification, in which MVs and thick abnormal collagen fibrils are potential nucleators in this process. Although this study documents changes in chondrocytes including apparent matrix accumulation of collagen, it was not

shown that it was causal for changes in chondrocyte differentiation and calcification.

Further, the clinical details suggest that this patient has a local rather than a systemic process and therefore it could be argued that it would be less likely that calcification is related to a genetic collagen abnormality. However, this being said, it is also noteworthy again to mention that abnormal type II collagen hetero-fibrils and pro-collagen accumulation were described for this patient's phenotype which are similar to findings in certain human type II collagenopathies [30] [31] [32], OCD [27] and patella alta/trochlea dysplasia [28].

This case report including control cartilage further supports the fact that chondrocyte hypertrophy is a key factor in articular cartilage calcification and the reported ERSD phenotype might contribute new reference points which could be important in understanding calcification in OA and other cartilage disease.

## Acknowledgements

This work was supported in part by Interface Biotech, 2790 Hørsholm, Denmark. The authors gratefully acknowledge Dr. David (Taff) Jones for reviewing the document.

## Conflicts of Interest

The authors declare no conflicts of interest regarding the publication of this paper.

## References

- [1] Fuerst, M., Bertrand, J., Lammers, L., Dreier, R., Echtermeyer, F., Nitschke, Y., Rutsch, F., Schäfer, F.K., Niggemeyer, O., Steinhagen, J., Lohmann, C.H., Pap, T. and Rüter, W. (2009) Calcification of Articular Cartilage in Human Osteoarthritis. *Arthritis & Rheumatism*, **60**, 2694-2703. <https://doi.org/10.1002/art.24774>
- [2] Fuerst, M., Lammers, L., Schäfer, F., Niggemeyer, O., Steinhagen, J., Lohmann, C.H. and Rüter, W. (2009) Investigation of Calcium Crystals in OA Knees. *Rheumatology International*, **30**, 623-631. <https://doi.org/10.1007/s00296-009-1032-2>
- [3] Fuerst, M. (2014) Chondrocalcinosis. Clinical Impact of Intra-Articular Calcium Phosphate Crystals. *Zeitschrift für Rheumatologie*, **73**, 415-419.
- [4] Sun, Y., Mauerhan, D.R., Honeycutt, P.R., Kneisl, J.S., Norton, H.J., Zinchenko, N., Edward, N., Hanley, E.N. and Gruber, H.E. (2010) Calcium Deposition in Osteoarthritic Meniscus and Meniscal Cell Culture. *Arthritis Research & Therapy*, **12**, R56. <https://doi.org/10.1186/ar2968>
- [5] Gordon, G.V., Villanueva, T., Schumacher, H.R. and Gohel, V. (1984) Autopsy Study Correlation Degree of Osteoarthritis, Synovitis and Evidence of Articular Calcification. *The Journal of Rheumatology*, **11**, 681-686.
- [6] Scotchford, C.A., Vickers, M. and Ali, S.Y. (1995) The Isolation and Characterization of Magnesium Whitlockite Crystals from Human Articular Cartilage. *Osteoarthritis and Cartilage*, **3**, 79-94. [https://doi.org/10.1016/s1063-4584\(05\)80041-x](https://doi.org/10.1016/s1063-4584(05)80041-x)
- [7] Mitsuyama, H., Healey, R.M., Terkeltaub, R.A., Coutts, R.D. and Amiel, D. (2007)

Calcification of Human Articular Cartilage Is Primarily an Effect of Aging rather than Osteoarthritis. *Osteoarthritis and Cartilage*, **15**, 559-565.

<https://doi.org/10.1016/j.joca.2006.10.017>

- [8] Jones, A.C., Chuck, A.J., Arie, E.A., Green, D.J. and Doherty, M. (1992) Diseases Associated with Calcium Pyrophosphate Deposition Disease. *Seminars in Arthritis and Rheumatism*, **22**, 188-202. [https://doi.org/10.1016/0049-0172\(92\)90019-a](https://doi.org/10.1016/0049-0172(92)90019-a)
- [9] Resnick, D., Scavulli, J.F., Goergen, T.G., Genant, H.K. and Niwayama, G. (1977) Intra-Articular Calcification in Scleroderma. *Radiology*, **124**, 685-688. <https://doi.org/10.1148/124.3.685>
- [10] Steinbach, L.S. and Resnick, D. (2000) Calcium Pyrophosphate Dehydrate Crystal Deposition Disease: Imaging Perspectives. *Current Problems in Diagnostic Radiology*, **29**, 209-229.
- [11] Nalbant, S., Martinez, J.A., Kitumnuaypong, T., Clayburne, G., Sieck, M. and Schumacher Jr., H.R. (2003) Synovial Fluid Features and Their Relations to Osteoarthritis Severity: New Findings from Sequential Studies. *Osteoarthritis and Cartilage*, **11**, 50-54. <https://doi.org/10.1053/joca.2002.0861>
- [12] Rosenthal, A.K. (2007) Update in Calcium Deposition Diseases. *Current Opinion in Rheumatology*, **19**, 158-162.
- [13] Olmez, N. and Schumacher Jr., H.R. (1999) Crystal Deposition and Osteoarthritis. *Current Rheumatology Reports*, **1**, 107-111. <https://doi.org/10.1007/s11926-999-0006-4>
- [14] Anderson, H.C. (2003) Matrix Vesicles and Calcification. *Current Rheumatology Reports*, **5**, 222-226.
- [15] Anderson, H.C., Mulhall, D. and Garimella, R. (2010) Role of Extracellular Membrane Vesicles in the Pathogenesis of Various Diseases, Including Cancer, Renal Diseases, Atherosclerosis, and Arthritis. *Laboratory Investigation*, **90**, 1549-1557. <https://doi.org/10.1038/labinvest.2010.152>
- [16] Ali, S.Y. (1985) Apatite-Type Crystal Deposition in Arthritic Cartilage. *Scanning Electron Microscopy*, Pt. 4, 1555-1566.
- [17] Anderson, H.C. (1988) Mechanisms of Pathologic Calcification. *Rheumatic Disease Clinics of North America*, **14**, 303-319.
- [18] Derfus, B.A., Kurtin, S.M., Camacho, N.P., Kurup, I. and Ryan, L.M. (1996) Comparison of Matrix Vesicles Derived from Normal and Osteoarthritic Human Articular Cartilage. *Connective Tissue Research*, **35**, 391-396. <https://doi.org/10.3109/03008209609029209>
- [19] Derfus, B., Kranendonk, S., Camacho, N., Mandel, N., Kushnaryov, V., Lynch, K., *et al.* (1998) Human Osteoarthritic Cartilage Matrix Vesicles Generate Both Calcium Pyrophosphate Dihydrate and Apatite *in Vitro*. *Calcified Tissue International*, **63**, 258-262. <https://doi.org/10.1007/s002239900523>
- [20] Cheung, H.S., Kurup, I.V., Sallis, J.D. and Ryan, L.M. (1996) Inhibition of Calcium Pyrophosphate Dihydrate Crystal Formation in Articular Cartilage Vesicles and Cartilage by Phosphocitrate. *The Journal of Biological Chemistry*, **271**, 28082-28085. <https://doi.org/10.1074/jbc.271.45.28082>
- [21] Bjelle, A. and Sundén, G. (1971) Pyrophosphate Synovitis. Crystal Synovitis Caused by Calcium Pyrophosphatedihydrate (CPPL) as a Diagnostic Problem in Orthopedic Patients. *Acta Orthopaedica Scandinavica*, **42**, 131-141. <https://doi.org/10.3109/17453677108989033>
- [22] Williams, C.J., Considine, E.L., Knowlton, R., Reginato, A.J., Neumann, G., Harri-

- son, D., Buxton, P.G., Jimenez, S. and Prockop, D.J. (1993) Spondyloepiphyseal Dysplasia and Precocious Osteoarthritis in a Family with an Arg<sub>75</sub> →Cys Mutation in the COL2A1. *Human Genetics*, **92**, 499-505. <https://doi.org/10.1007/bf00216458>
- [23] Reginato, A.J., Passano, G.M., Neumann, G., Falasca, G.F., Diaz-Valdez, M., Jimenez, S.A. and Williams, C.J. (1994) Familial Spondyloepiphyseal Dysplasia Tarda, Brachydactyly, and Precocious Osteoarthritis Associated with an Arginine 75 →Cysteine Mutation in the Procollagen Type II Gene in a Kindred of Chiloe Islanders. *Arthritis & Rheumatism*, **37**, 1078-1086. <https://doi.org/10.1002/art.1780370714>
- [24] Bleasel, J.F., Bisagni-Faure, A., Holderbaum, D., Vacher-Lavenu, M.C., Haqqi, T.M., Moskowitz, R.W., et al. (1995) Type II Procollagen Gene (COL2A1) Mutation in Exon 11 Associated with Spondyloepiphyseal Dysplasia, Tall Stature and Precocious Osteoarthritis. *The Journal of Rheumatology*, **22**, 255-261.
- [25] Bleasel, J.F., Holderbaum, D., Mallock, V., Haqqi, T.M., Williams, H.J. and Moskowitz, R.W. (1996) Hereditary Osteoarthritis with Mild Spondyloepiphyseal Dysplasia: Are There "Hot Spots" on COL2A1? *The Journal of Rheumatology*, **23**, 1594-1598.
- [26] Löppönen, T., Körkkö, J., Lundan, T., Seppänen, U., Ignatius, J. and Kääriäinen, H. (2004) Childhood-Onset Osteoarthritis, Tall Stature, and Sensorineural Hearing Loss Associated with Arg<sup>75</sup>-Cys Mutation in Procollagen Type II Gene (COL2A1). *Arthritis Care & Research*, **51**, 925-932. <https://doi.org/10.1002/art.20817>
- [27] Skagen, P.S., Horn, T., Kruse, H.A., Staergaard, B., Rapport, M.M. and Nicolaisen, T. (2011) Osteochondritis Dissecans (OCD), an Endoplasmic Reticulum Storage Disease?: A Morphological and Molecular Study of OCD Fragments. *Scandinavian Journal of Medicine & Science in Sports*, **21**, e17-e33. <https://doi.org/10.1111/j.1600-0838.2010.01128.x>
- [28] Skagen, P.S., Horn, T., Milunsky, A., Dejour, D., Stærgaard, B., Aagaard Kruse, H. and Nicolaisen, T. (2014) Patella Alta and Trochlea Dysplasia is Associated with Abnormal Type II Collagen and Matrix Accumulation in Chondrocytes. *Microscopy Research*, **2**, 19-29. <https://doi.org/10.4236/mr.2014.22004>
- [29] Balcerzak, M., Radisson, J., Azzar, G., Farlay, D., Boivin, G., Pikula, S. and Buchet, R. (2007) A Comparative Analysis of Strategies for Isolation of Matrix Vesicles. *Analytical Biochemistry*, **361**, 176-182. <https://doi.org/10.1016/j.ab.2006.10.001>
- [30] Nishimura, G., Haga, N., Kitoh, H., Tanaka, Y., Sonoda, T., Kitamura, M., Shirahama, S., Itoh, T., Nakashima, E., Ohashi, H. and Ikegawa, S. (2005) The Phenotypic Spectrum of COL2A1 Mutations. *Human Mutation*, **26**, 36-43. <https://doi.org/10.1002/humu.20179>
- [31] Spranger, J., Winterpacht, A. and Zabel, B. (1994) The Type II Collagenopathies: A Spectrum of Chondrodysplasias. *European Journal of Pediatrics*, **153**, 56-65. <https://doi.org/10.1007/bf01959208>
- [32] Horton, W.A. and Rimoin, D.L. (1979) Kniest Dysplasia. A Histochemical Study of the Growth Plate. *Pediatric Research*, **13**, 1266-1270. <https://doi.org/10.1203/00006450-197911000-00012>
- [33] Hintze, V., Steplewski, A., Ito, H., Jensen, D.A., Rodeck, U. and Fertala, A. (2008) Cells Expressing Partially Unfolded R789C/p.R989C Type II Procollagen Mutant Associated with Spondyloepiphyseal Dysplasia Undergo Apoptosis. *Human Mutation*, **29**, 841-851. <https://doi.org/10.1002/humu.20736>
- [34] Rick, A. and Crick, F.H. (1961) The Molecular Structure of Collagen. *Journal of Molecular Biology*, **3**, 483-506.
- [35] Yang, C., Li, S.W., Helminen, H.J., Khillan, J.S., Bao, Y. and Prockop, D.J. (1997)

- Apoptosis of Chondrocytes in Transgenic Mice Lacking Collagen II. *Experimental Cell Research*, **235**, 370-373. <https://doi.org/10.1006/excr.1997.3692>
- [36] Van der Eerden, B.C., Karperien, M. and Wit, J.M. (2003) Systemic and Local Regulation of the Growth Plate. *Endocrine Reviews*, **24**, 782-801. <https://doi.org/10.1210/er.2002-0033>
- [37] Anderson, H.C. (1969) Vesicles Associated with Calcification in the Matrix of Epiphyseal Cartilage. *The Journal of Cell Biology*, **41**, 59-72.
- [38] Anderson, H.C. (1990) Biology of Disease—Mechanism of Mineral Formation in Bone. In: Rubin, E. and Damjanov, I., Eds., *Pathology Reviews*, The Humana Press Inc., Clifton, NJ, 13-23.
- [39] Cui, L., Houston, D.A., Farquharson, C. and MacRae, V.E. (2016) Characterisation of Matrix Vesicles in Skeletal and Soft Tissue Mineralisation. *Bone*, **87**, 147-158. <https://doi.org/10.1016/j.bone.2016.04.007>
- [40] Hunter, G.K. (1987) An Ion-Exchange Mechanism of Cartilage Calcification. *Connective Tissue Research*, **16**, 111-120.
- [41] Hunter, G.K. (1991) Role of Proteoglycan in the Provisional Calcification of Cartilage. A Review and Reinterpretation. *Clinical Orthopaedics and Related Research*, No. 262, 256-280.
- [42] Poole, A.R. (1991) The Growth Plate: Cellular Physiology, Cartilage Assembly and Mineralization. In: Hall, B. and Newman, S., Eds., *Cartilage: Molecular Aspects*, CRC Press, Boca Raton, FL, 179-211.
- [43] Kirsch, T., Nah, H.D., Shapiro, I.M. and Pacifici, M. (1997) Regulated Production of Mineralization-Competent Matrix Vesicles in Hypertrophic Chondrocytes. *The Journal of Cell Biology*, **137**, 1149-1160. <https://doi.org/10.1083/jcb.137.5.1149>
- [44] Kirsch, T. (2006) Determinants of Pathological Mineralization. *Current Opinion in Rheumatology*, **18**, 174-180.
- [45] Borg, T.K., Runyan, R.B. and Wuthier, R.E. (1978) Correlation of Freeze-Fracture and Scanning Electron Microscopy of Epiphyseal Chondrocytes. *Calcified Tissue Research*, **26**, 237-241. <https://doi.org/10.1007/bf02013264>
- [46] Anderson, H.C. (1995) Molecular Biology of Matrix Vesicles. *Clinical Orthopaedics and Related Research*, No. 314, 266-280.
- [47] Wuthier, R.E. and Lipscomb, G.F. (2011) Matrix Vesicles: Structure, Composition, Formation and Function in Calcification. *Frontiers in Bioscience*, **16**, 2812-2902. <https://doi.org/10.2741/3887>
- [48] Glimcher, M. (1989) Mechanisms of Calcification in Bone: Role of Collagen Fibrils and Collagen-Phosphoprotein Complexes *in Vitro* and *in Vivo*. *The Anatomical Record*, **224**, 139-153. <https://doi.org/10.1002/ar.1092240205>
- [49] Tong, W., Glimcher, M.J., Katz, J.L., Kuhn, L. and Eppell, S.J. (2003) Size and Shape of Mineralites in Young Bovine Bone Measured by Atomic Force Microscopy. *Calcified Tissue International*, **72**, 592-598. <https://doi.org/10.1007/s00223-002-1077-7>
- [50] Halverson, P.B., Greene, A. and Cheung, H.S. (1998) Intracellular Calcium Responses to Basic Calcium Phosphate Crystals in Fibroblasts. *Osteoarthritis and Cartilage*, **6**, 324-329. <https://doi.org/10.1053/joca.1998.0131>
- [51] Beutler, A., Rothfuss, S., Clayburne, G., Sieck, M. and Schumacher Jr., H.R. (1993) Calcium Pyrophosphate Dihydrate Crystal Deposition in Synovium. Relationship to Collagen Fibers and Chondrometaplasia. *Arthritis & Rheumatism*, **36**, 704-715. <https://doi.org/10.1002/art.1780360520>
- [52] McCarty, D.J. (1974) Crystal Deposition Joint Disease. *Annual Review of Medicine*,

**25**, 279-288.

- [53] Van der Rest, M., Rosenberg, L.C., Olsen, B.R. and Poole, A.R. (1986) Chondrocalcin Is Identical with the C-Propeptide of Type II Collagen. *Biochemical Journal*, **237**, 923-925. <https://doi.org/10.1042/bj2370923>